Inorganica Chimica Acta 518 (2021) 120220

Contents lists available at ScienceDirect

Inorganica Chimica Acta

journal homepage: www.elsevier.com/locate/ica

Research paper

Homodinuclear organometallics of ditopic *N,N*-chelates: Synthesis, reactivity and *in vitro* anticancer activity

Tasha R. Steel [a], Kelvin K.H. Tong [a], Tilo Söhnel [a], Stephen M.F. Jamieson [b], L. James Wright [a], James D. Crowley [c], Muhammad Hanif [a,*,1], Christian G. Hartinger [a,*,1]

[a] School of Chemical Sciences, University of Auckland, Private Bag 92019, Auckland 1142, New Zealand
[b] Auckland Cancer Society Research Centre, University of Auckland, Private Bag 92019, Auckland 1142, New Zealand
[c] Department of Chemistry, University of Otago, PO Box 56, Dunedin, New Zealand

ARTICLE INFO

Dedicated to Prof. Maurizio Peruzzini on the occasion of his 65th birthday.

Keywords:
Bioorganometallics
Cancer chemotherapy
Ditopic ligands
Polynuclear complexes

ABSTRACT

In some instances, multimetallic complexes have shown higher anticancer activity than mononuclear analogues, possibly by interacting with target molecules through a different binding mode. Therefore, a series of novel bis-pyridylimine-based homodinuclear $M^{II/III}$(cym/Cp*)Cl (cym = η^6-*p*-cymene: M = Ru, Os; Cp* = η^5-pentamethylcyclopentadienyl: M = Rh, Ir) complexes were synthesized and studied. The dinuclear complexes were characterized by ^{1}H, ^{13}C{^{1}H}, and ^{31}P{^{1}H} NMR spectroscopy, ESI-MS, and elemental analysis. Additionally, the molecular structures of several complexes were investigated by single crystal X-ray diffraction analysis. [{*N*,*N*'-(1,4-Phenylene)(bis(1-(pyridin-2-yl)(methanimine)-κ^2*N*,*N*'))}bis{chlorido(η^6-*p*-cymene)ruthenium(II)}] hexafluorophosphate, **1a**, was used in stability and binding studies to 9-ethylguanine (EtG) as a DNA nucleobase model and L-histidine (His), L-cysteine (Cys) and L-methionine (Met) as protein models. However, compared to structurally related Ru(arene) complexes, the investigations were inconclusive in terms of the nature of hydrolysis product(s) and EtG adducts formed, while reactions to His and Cys but not Met were observed for **1a**. The *in vitro* cytotoxicity of the ligands and dinuclear complexes was determined against a small panel of human cancer cell lines. Some of the complexes showed moderate antiproliferative activity but were less potent than the bis-pyridylimine-based bridging ligands.

1. Introduction

The field of medicinal inorganic chemistry gained significant momentum after the serendipitous discovery of the cytotoxic properties of the platinum-based complex cisplatin [1–3]. Although several successful new generations of cisplatin derivatives have since been developed, traditional platinum-based chemotherapy is commonly associated with severe dose-limiting side effects and drug resistance, either acquired or intrinsic [4–9]. As a result, research efforts have sought alternative treatment options and focus has turned to complexes formed from a variety of other transition metals [3,10].

Incorporating multiple transition metal centers in inorganic anticancer agents has in several cases shown an improvement in anticancer activity when compared to their monometallic analogues [11–14]. One such compound is the tri-nuclear Pt complex BBR3464 which showed superior *in vitro* and *in vivo* activity compared to cisplatin in cisplatin-resistant cancer models, probably because of alternative DNA interaction modes [15]. However, BBR3464 was found to be toxic to patients with gastric or gastro-esophageal adenocarcinomas in a phase II clinical trial [16]. The concept of multinuclearity has been developed further to include Ru [12,14,17–22] Au [19,23,24] Fe [25] and Ti [26] centers in homo- and heteromultimetallic complexes, affording diverse mechanisms of action.

We have previously reported a series of dinuclear Ru^{II}(arene) anticancer agents with *in vitro* anticancer activity dependent on the length of the aliphatic linker, where 1,12-bis{chlorido[3-(oxo-κ*O*)-2-methyl-4-pyridinonato-κ*O*](η^6-*p*-cymene)ruthenium(II)}dodecane (**Ru_2**) was the most potent derivative [17,18,21,27]. These dinuclear Ru^{II}(arene) compounds underwent fast chlorido/aqua ligand exchange in aqueous solution, and were able to bind to both proteins and DNA [18]. A notable feature of their mode of action was that they cross-linked DNA duplexes as well as DNA and proteins [27]. The same ditopic pyridone-based

* Corresponding authors.
E-mail addresses: m.hanif@auckland.ac.nz (M. Hanif), c.hartinger@auckland.ac.nz (C.G. Hartinger).
[1] http://hartinger.auckland.ac.nz/.

https://doi.org/10.1016/j.ica.2020.120220
Received 15 September 2020; Received in revised form 13 December 2020; Accepted 17 December 2020
Available online 12 January 2021

ligand system was used to prepare Rh(Cp*)Cl and Ir(Cp*)Cl analogues (**Rh_2** and **Ir_2**), which resulted in similar or superior cytotoxic activity compared to the Ru analogue. **Rh_2** was slightly more active than the **Ru_2** and **Ir_2** counterparts with IC_{50} values of *ca.* 50 nM in non-small cell lung carcinoma NCI-H460 cells. **Rh_2** and **Ir_2** showed DNA damaging ability similar to **Ru_2** as well as cisplatin [28,29], while both were capable of inducing the formation of reactive oxygen species in cancer cells. Importantly, they were found to be less toxic than cisplatin in hemolysis and *in vivo* zebrafish assays whilst retaining cytotoxicity [29]. Other examples include dinuclear Ru compounds based on *N,N'*-bis(2-aminoethyl)-hexane-1,6-diamine linkers with biphenyl arene moieties which have shown *in vitro* anticancer activity similar to or lower than the mononuclear analogues towards A2780 ovarian cancer cells [30].

In line with our interest in designing multinuclear metal complexes for biological applications, we report the synthesis and characterization of a series of homodinuclear metal complexes of two different ditopic pyridylimine ligands. We also report the investigation of aqueous and DMSO stability, reactivity towards biomolecules and *in vitro* cytotoxic properties.

2. Results and discussion

Ligands featuring the pyridylimine coordination motif have been widely studied due to their extreme versatility, accessible syntheses, and formation of stable coordination complexes with many transition metals [31]. Additionally, several pyridylimine transition metal complexes have shown promising biological and anticancer activity [32–37]. The syntheses of bis-pyridylimine ligands **1** and **2** (Scheme 1) followed modified literature preparations using condensation reactions of 2-pyridine carboxaldehyde (2 equiv.) with 1,4-diaminobenzene or 4,4′-methylene dianiline (1 equiv.), respectively [38,39]. These ditopic ligands with a bidentate *N,N*-chelating group at each coordination pocket were employed to prepare a series of homodimetallic complexes. Complexes **1a**–**1d** and **2a**–**2d** were obtained by adding **1** or **2** (1 equiv.) to stirred solutions of the dimeric metal precursors $[M^{II/III}(cym/Cp^*)Cl_2]_2$ **a**–**d** (1 equiv.) in dichloromethane (DCM)/methanol (MeOH) (1:1) at room temperature (r.t.) for *ca.* 20 h. Following anion exchange using excess NH_4PF_6, the homodimetallic complexes **1a**–**1d** and **2a**–**2d** were obtained as pure solids in good to excellent yields (73–95%) (Scheme 1). Complex **$1a^{Cl}$**, an analogue of **1a** which retains the chloride counteranions [37], and the tetrafluoroborate derivative (**$1a^{BF4}$**) [40] have been reported previously.

Characterization of the homodinuclear complexes was achieved through analysis of ^1H, $^{31}P\{^1H\}$ and $^{13}C\{^1H\}$ NMR spectroscopic data (Supporting Information) as well as electrospray ionization mass spectrometry (ESI-MS) and elemental analysis. The ^1H NMR spectra revealed the expected peaks originating from the cym/Cp* moieties and the bis-pyridylimine ligands. The signals assigned to the protons of the central phenylene ring(s) appeared as distinct singlets at *ca.* 8.1 ppm for complexes **1a**–**1d** (H-6) and as two doublets at *ca.* 7.6 ppm for complexes **2a**–**2d** (H-6/7), due to the presence of the methylene group in the latter. Protons H-1 and H-5 adjacent to the endocyclic nitrogen atoms of the bis-pyridylimine ligands saw the most significant downfield shifts upon coordination of the ligands to the corresponding metal centers, appearing for all complexes between *ca.* 8.9 and 9.6 ppm. For complexes containing the Cp* moiety, the methyl groups appeared as a singlet at around 1.6 ppm. Exchange of the chloride counterions for hexafluorophosphate (PF_6^-) was indicated by $^{31}P\{^1H\}$ NMR spectroscopy,

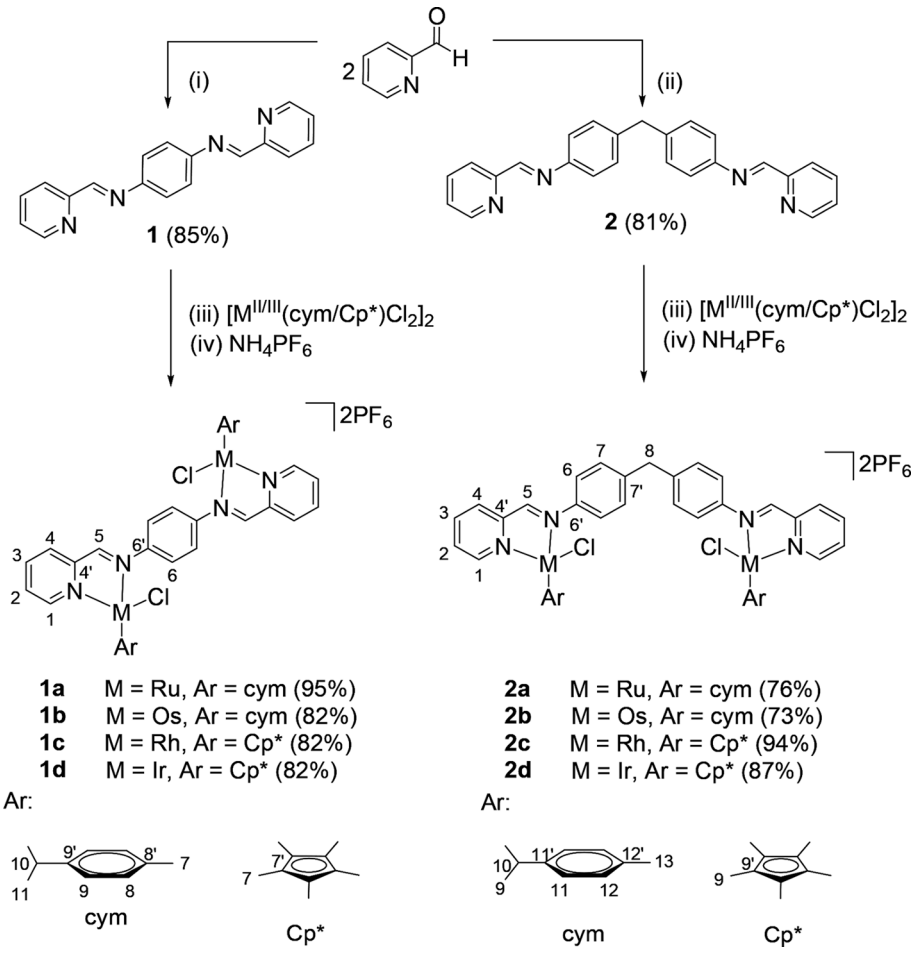

Scheme 1. Preparation of dinuclear $[\{M^{II/III}(cym/Cp^*)Cl\}_2(pyridylimine\ ligand\ \mathbf{1/2})]PF_6$ complexes **1a**–**1d** and **2a**–**2d**, as well as the ^1H and $^{13}C\{^1H\}$ NMR numbering scheme used. Conditions: (i) 1,4-diaminobenzene, EtOH, 20 h, reflux; (ii) 4,4′-methylene dianiline, MeOH, 20 h, r.t.; (iii) $[M^{II/III}(cym/Cp^*)Cl_2]_2$, DCM : MeOH, 20 h, r.t.; (iv) NH_4PF_6, MeOH, 1 h, r.t. The syntheses of ligands **1** and **2** have been previously reported [38,39] as well as those of the analogous complexes **$1a^{Cl}$** and **$1a^{BF4}$** [37,40].

where a septet at *ca.* –140 ppm was observed for all complexes.

ESI-mass spectra recorded in positive ionization mode generated base peaks that corresponded to $[M - 2PF_6]^{2+}$ cations for complexes **1a**, **1b**, and **2a**–**2d**. In contrast, the base peaks for complexes **1c** and **1d** were found as the singly charged mononuclear Rh^{III}/Ir^{III} species following hydrolysis at one of the Schiff bases and subsequent loss of a metal center, pyridyl unit and chlorido ligand during MS analysis to give cations assignable to $[M - C_6H_5N - Rh/Ir(Cp^*)Cl - 2PF_6]^+$.

The molecular structures of **1b**–**1d**, **2a** and **2c** were determined by single crystal X-ray diffraction analysis (Table S1). Single crystals were grown by the slow diffusion of toluene into saturated solutions of the respective complex in acetonitrile. All complexes display the characteristic pseudooctahedral piano-stool configuration around the metal centers, with the pyridylimine and Cl ligands forming the legs of the stool and the π-bound cym or Cp* rings acting as the seat *via* η^6- or η^5-coordination, respectively. Complexes **1b**–**1d**, and **2c** crystallized as mixtures of enantiomers with both metal centers in each molecule having the same configuration. In contrast, the two metal centers in each molecule of **2a** had opposite configurations. Complexes **1b**–**1d** adopted a triclinic crystal system and crystallized in the *P*-1 space group (Fig. 1, Fig. S1 for **1d**). Complexes **2a** and **2c** adopted a monoclinic crystal system in the *I*2/*a* space group (Fig. 2, Table S1). The presence of a five-membered ring, that forms upon metal coordination, confirms the *N,N*-bidentate coordination mode of the bis-pyridylimine chelate ligands in **1b**–**1d** (as well as for **2a** and **2c**), which was also observed for the tetrafluoroborate derivative of **1a**, *i.e.*, $\mathbf{1a}^{BF4}$ [40]. Epimerization can occur in complexes closely related to these through chlorido ligand dissociation and re-coordination on the opposite side of the metallacyclic ring to form a mixture of isomers in solution [41]. The presence of a single set of peaks in the ^{1}H NMR spectrum suggests that the epimerization process is fast relative to the ^{1}H NMR timescale.

The two Cp* rings in each of the complexes **1c** and **1d** sit on opposite sides of the bridging phenylene group in the solid state structures,

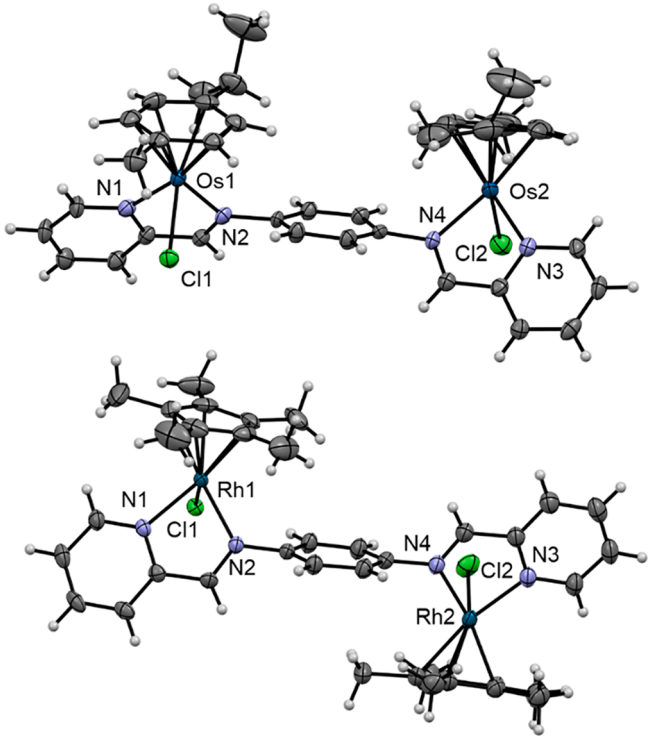

Fig. 1. ORTEP representations of one of the molecules of the complex cations of **1b** (top) and **1c** (bottom) drawn at 50% probability levels. Co-crystallized solvent molecules, and hexafluorophosphate counteranions have been omitted for clarity.

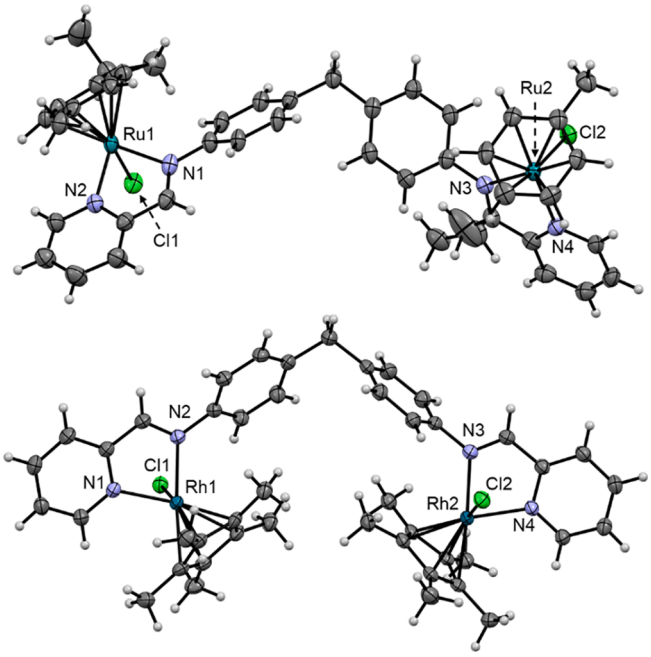

Fig. 2. ORTEP representations of one of the molecules of the complex cations **2a** (top) and **2c** (bottom) drawn at 50% probability levels. Co-crystallized solvent molecules, and hexafluorophosphate counteranions have been omitted for clarity.

although the NMR data suggest that in solution rotation occurs rapidly about the N2-C(X) and N4-C(Y) bonds. The pyridylimine units are not co-planar to the central phenylene ring and have torsion angles of −60.38 and −72.95° for **1c**, and −106.72 and +60.85° for **1d**. These angles are presumably determined by a combination of steric repulsions, π-bond formation with the phenylene unit, intermolecular interactions and crystal packing forces. A similar molecular geometry was reported for structurally related dinuclear Ru complex $\mathbf{1a}^{BF4}$ [40]. In contrast, the two cym rings in the solid state structure of the di-osmium derivative **1b** were oriented on the same side of the bridging phenylene group, in a staggered geometry. The torsion angles between the pyridylimine units and the central phenylene ring are +48.21 and +48.40° for **1b**. In general, the other aspects of the structures do not differ significantly upon altering the metal center. The differences in metal–ligand bond lengths of **1b**–**1d** are no greater than 0.01, 0.05 and 0.02 Å for the M1–Cl1, M1–$N_{pyridyl}$ and M1–N_{imine} bonds, respectively (Table 1), and the interatomic distance between the two metal centers (M1···M2) was calculated to be *ca.* 8.4 Å. The M−Cl bond lengths were very close to the average values for these types of complexes [42]. π-Stacking between the cym ring of one molecule of Os complex **1b** and the phenylene bridge of another was found at 3.35 Å.

Table 1
Key bond lengths (Å) and angles (°) in the molecular structures of complexes **1b**–**1d**, **2a**, and **2c**, in comparison to $\mathbf{1a}^{BF4}$.

Bond/ angle	$\mathbf{1a}^{BF4}$ [a]	1b	1c	1d	2a	2c
M1–Cl1	2.3863 (14)	2.3991 (15)	2.4082 (7)	2.4096 (8)	2.3972 (14)	2.4050 (5)
M1–N1	2.099 (4)	2.079 (5)	2.125 (2)	2.106 (3)	2.099 (4)	2.104 (2)
M1–N2	2.055 (4)	2.087 (5)	2.110 (2)	2.090 (3)	2.077 (4)	2.113 (2)
N1–M1–N2	76.50 (14)	76.0(2)	76.51 (9)	76.18 (11)	76.84 (17)	77.09 (7)

[a] Taken from Ref. [40].

Complex **2c** with the central methylene bridge is structurally flexible and its Cp* units sit on the same internal face of ligand **2**. The distances between the two metal centers were found to be *ca.* 13.3 and 9.2 Å for complexes **2a** and **2c**, respectively, and were therewith significantly greater than for complexes of **1**. There were only slight differences in the torsion angles involving the diphenylmethylene moieties and in the metal–ligand bond lengths. In the structure of **2a**, intermolecular π-interactions between the terminal pyridyl rings of adjacent molecules were found at 3.38 Å.

2.1. Stability studies in dimethylsulfoxide and aqueous solution

Many transition metal complexes undergo aquation under physiological conditions, *i.e.*, halido/aqua ligand exchange, which is important for facilitating metal binding to biomolecular targets [43,44]. However, many organometallic complexes have low aqueous solubility and therefore, in these cases, biological assays usually require prior dissolution of the complex in a water-miscible solvent such as dimethylsulfoxide (DMSO). A complication of using DMSO as a solvent is that it has the ability to coordinate to metal centers, for example, through halido ligand exchange, and this may alter the structure and nature of the pharmacophore and sometimes even lead to decomposition [45]. Consequently, preliminary ^{1}H NMR spectroscopic studies were conducted for **1a** in 10% DMSO-d_6/D_2O as a representative example over a period of 72 h (Fig. S2). In particular, we were interested in whether any evidence could be obtained that indicated the M−$N_{pyridyl}$ and M−N_{imine} bonds were retained during this time. Unfortunately, **1a** had low solubility in this solvent mixture and furthermore, a small amount of precipitate formed in the NMR tube over the timeframe of analysis. These factors resulted in a low signal-to-noise ratio in the ^{1}H NMR spectra, especially those taken after 24 h. Comparison of these spectra with those taken of **1a** in the presence of 100 mM NaCl in 10% DMSO-d_6/D_2O (to suppress chlorido/aqua ligand exchange), or those taken after the addition of 2 equiv. $AgNO_3$ in 10% DMSO-d_6/D_2O, (to remove the chlorido ligand as AgCl) showed almost no differences between them at all (Fig. S2). It is reasonable to assume the same product was formed in each case, and this is most likely to be a derivative of **1a** in which both metal-bound chlorido ligands have been replaced either by DMSO, aqua or hydroxido ligands. Formation of a derivative with aqua ligands is less likely as this would result in a quadruply-charged complex for which spontaneous deprotonation of the aqua ligands would be expected to readily occur to give less labile hydroxido ligands [46]. In summary, on the basis of the limited changes observed in the NMR spectra described above, we assume that any substitution product of complex **1a** formed immediately upon dissolution and showed reasonable stability for 72 h under the conditions investigated. The results indicate that, in biologically relevant solutions, the complexes retain their structural integrity with the M−$N_{pyridyl}$, M−N_{imine} and M−arene/Cp* bonds remaining intact. Therefore, this was sufficient to allow for biological assays to be carried out (Figs. S2 and S3).

2.2. Biomolecule interaction

Many metal complexes are known to covalently bind to DNA, where the nucleophilic *N*7 atom of guanine is often a preferential binding site [47–50]. The potential for **1a** to bind to DNA over 72 h was assessed by ^{1}H NMR spectroscopy using 9-ethylguanine (EtG) as a model compound in a **1a**:EtG ratio of 1:2 in 10% DMSO-d_6/D_2O (Figs. S4 and S5). Any chlorido/aqua/DMSO exchange that occurred could lead to activation of **1a** for biomolecule coordination and may allow for formation of **1a**–EtG adducts. In contrast, a hydroxido complex may be more inert towards further substitution with EtG. The most prominent indication of EtG binding to a metal center is usually the downfield shift of the signal assigned to H-8 of EtG [51]. In this case, upon addition of EtG to **1a**, a downfield shift of only *ca.* 0.09 ppm was immediately observed. However, addition of a further 2 equiv. of EtG to this sample did not yield a secondary peak pertaining to the H-8 of unbound EtG. Instead, a precipitate formed that gave a ^{1}H NMR spectrum identical to that of **1a**. Titration of EtG with DCl resulted in the H-8 signal of EtG to shift to lower field, with the shift dependent on the amount of DCl added. This may point to the possible formation of hydroxido ligands that prevent binding of EtG to **1a**.

Furthermore, we investigated the reaction of **1a** with the amino acids L-methionine (Met), L-histidine (His) and L-cysteine (Cys) in 10% DMSO-d_6/D_2O by ^{1}H NMR spectroscopy (data not shown). Similar behavior as in the stability studies with DMSO-d_6/D_2O was observed in the reaction between **1a** and Met. The spectra recorded in the first 2 h of the reaction were virtually unchanged compared to those of **1a**, but after 72 h minor peaks at around 9.0 and 9.8 ppm were observed, while only minor changes in the region indicative of the cym protons were detected. In case of Cys and His, more significant changes in the ^{1}H NMR spectra were observed. Similar to Met, in case of reaction with Cys, the cym protons did not change significantly, which is unusual as cym complexes often decompose in the presence of Cys [52,53]. Moreover, additional signals in the aromatic and aliphatic regions of the spectra indicated coordination of Cys. Similarly, the reaction with His resulted in significant changes in the peak pattern in the aromatic region.

2.3. In vitro cytotoxic activity

Ligands **1** and **2**, and complexes **1a**–**1d** and **2a**–**2d** were subjected to a sulforhodamine B cytotoxicity assay in the human cancer cell lines HCT116 (colorectal carcinoma), NCI-H460 (non-small cell lung carcinoma), SiHa (cervical carcinoma), and SW480 (colon adenocarcinoma) (Table 2). Compounds that gave mean half maximal inhibitory concentrations (IC_{50}) of >100 μM were deemed to be inactive in that particular cell line. In most cell lines, ligands **1** and **2** showed better antiproliferative properties than their corresponding metal complexes. Complex **1c** was the only derivative of **1** with IC_{50} values less than 100 μM in all cell lines under the conditions used. Complexes **2a** and **2b** showed minor activity only in SiHa and NCI-H460 cells, respectively, whereas **2c** and **2d** showed activity in all cell lines except NCI-H460. **2c** and **2d** were most potent in SiHa cells with IC_{50} values of 44 ± 1 and 45 ± 4 μM, respectively. Notably, both Rh-based complexes **1c** and **2c** showed moderate activity in almost all cell lines, while only the Ir complex of **2**, *i.e.*, **2d**, was moderately active.

3. Conclusions

A series of homodinuclear $M^{II/III}$(cym/Cp*)Cl complexes derived from ditopic pyridylimine ligands have been synthesized. The syntheses

Table 2
IC_{50} values (μM) for ligands **1** and **2** and complexes **1a**–**1d** and **2a**–**2d** against HCT116 (human colorectal carcinoma), NCI-H460 (human non-small cell lung carcinoma), SiHa (human cervical carcinoma), and SW480 (human colon adenocarcinoma) cancer cells as compared to cisplatin, expressed as mean ± standard error (n = 3).

Compound	HCT116	NCI-H460	SiHa	SW480
		IC_{50}/μM		
1	55 ± 20	57 ± 6	88 ± 4	>100
2	21 ± 6	31 ± 4	42 ± 3	46 ± 5
1a	>100	>100	>100	>100
1b	>100	>100	>100	>100
1c	70 ± 29	61 ± 13	70 ± 1	73 ± 4
1d	>100	>100	>100	>100
2a	>100	>100	83 ± 23	>100
2b	>100	81 ± 6	>100	>100
2c	78 ± 21	>100	44 ± 1	52 ± 9
2d	59 ± 31	>100	45 ± 4	73 ± 5
cisplatin[a]	2.5 ± 0.3	0.8 ± 0.03	3.0 ± 0.6	8.1 ± 2.9

[a] Taken from Ref. [54].

were facile and generated pure products in high yields. All complexes were characterized by 1D and 2D NMR spectroscopy, ESI-MS, and elemental analysis. Single crystals of complexes **1b**–**1d**, **2a**, and **2c** were analyzed by X-ray diffraction crystallography for structural validation. The complexes crystallized as a mixture of isomers with the molecules showing a variety of conformations, depending on both the ligand structures and the metal center. In **1c** and **1d**, the Cp* rings sat on opposite sides of **1**, while in the structure of **1b** both cym rings were arranged on the same side of **1**. Stability studies conducted as a prelude for biological experiments indicated that complex **1a**, or a rapidly formed hydrolysis product, was adequately stable in 10% DMSO-d_6/D_2O and DMSO-d_6 over a period of 72 h. Surprisingly, studies on the reactivity with the DNA model EtG were inconclusive, while **1a** formed adducts with Cys and His but not with Met. The *in vitro* cytotoxicity assays demonstrated limited cytotoxicity of the homodinuclear complexes with the ligands being more potent than the derived complexes. However, the Rh and Ir complexes **2c** and **2d** showed the best antiproliferative effect toward human cervical carcinoma cells, despite at moderate IC_{50} values compared to the anticancer drug cisplatin.

4. Experimental section

4.1. Materials and methods

All air and moisture-sensitive reactions were carried out under a nitrogen (N_2) atmosphere, and light sensitive reactions were protected from photolytic degradation by covering the apparatus in aluminum foil. Chemicals and solvents purchased from commercial suppliers were used without further purification. Solvents were dried prior to use when necessary. Solvents were evaporated under reduced pressure using a rotary evaporator. The precursor complexes $[RuCl_2(cym)]_2$ (**a**) [55], $[OsCl_2(cym)]_2$ (**b**) [56], $[RhCl_2(Cp^*)]_2$ (**c**) [57,58], and $[IrCl_2(Cp^*)]_2$ (**d**) [57,59], as well as the pyridylimine ligands **1** and **2** were prepared according to literature procedures [38,39].

Both 1D (^{1}H, and ^{13}C{^{1}H}DEPT-Q, ^{31}P{^{1}H}) and 2D (^{1}H–^{1}H COSY, ^{1}H–^{1}H NOESY, ^{1}H^{13}C HSQC, ^{1}H–^{13}C HMBC) NMR spectra were recorded on Bruker DRX 400 MHz NMR spectrometers at ambient temperature. The measurement frequencies for ^{1}H, ^{13}C{^{1}H}, and ^{31}P{^{1}H} NMR were 399.89, 100.55 and 161.85 MHz, respectively. Deuterated chloroform, acetone-d_6, D_2O, and DMSO-d_6 were used as NMR solvents. High resolution mass spectrometry (HRMS) data were recorded on a Bruker microTOF-Q II mass spectrometer in positive ion electrospray ionization (ESI) mode. Melting and decomposition points were recorded on a Stuart SMP50 automatic melting point apparatus. X-ray diffraction measurements of single crystals were conducted on a Rigaku Oxford Diffraction XtaLAB Synergy-S single-crystal diffractometer with a PILATUS 200 K hybrid pixel array detector using Cu Kα radiation (λ = 1.54184 Å). The structure solution and refinements were performed with the SHELXS-97, SHELXL-2016 [60] and Olex2 program packages [61,62]. Molecular structures were visualized using Mercury 4.0.0. Elemental analyses (EA) were carried out on the vario EL cube CHNOS Elemental analyzer at the University of Auckland for Ru, Rh, and Ir complexes, and at the Campbell Microanalytical Laboratory, the University of Otago for Os complexes.

4.2. General procedure for the synthesis of homodinuclear complexes *1a*–*1d* and *2a*–*2d*

Pyridylimine ligands **1** or **2** (1.0 equiv.) were added to a solution of dimeric metal precursor complex (**a**–**d**, 1.0 equiv.) in DCM : MeOH (60 mL, 1 : 1) and stirred at r.t. overnight. The solvent was removed under reduced pressure. The crude product was dissolved in MeOH (20 mL) and a solution of NH_4PF_6 (20 equiv.) in MeOH (20 mL) was added. The resulting mixture was stirred for 1 h, was concentrated under reduced pressure and chilled overnight. The precipitate was filtered, washed with cold MeOH, and dried. The crude product was dissolved in DCM (40 mL), filtered and the solvent removed from the filtrate under reduced pressure. However, in the case of complex **1b**, the crude product was dissolved in DCM : acetone (1 : 1, 40 mL), filtered, and the solvent was removed under reduced pressure. The resulting residue was dried *in vacuo* to obtain pure complexes in high yields.

4.3. [N,N'-(1,4-phenylene)(bis(1-(pyridin-2-yl)(methanimine)-κ^{2}N,N') bis{chlorido(η^6-p-cymene)ruthenium(II)}] hexafluorophosphate *1a*

The synthesis was performed according to the general procedure using **1** (104 mg, 0.36 mmol), $[RuCl_2(cym)]_2$ (244 mg, 0.36 mmol), and NH_4PF_6 (1.174 g, 7.2 mmol) to afford the product **1a** as an orange solid (387 mg, 95%). M.p. 220 °C (decomp.). ^{1}H NMR (399.89 MHz, acetone-d_6, *298 K*): δ 9.56 (d, ^3J = 3 Hz, 2H, H-1), 8.93 (s, 2H, H-5), 8.34–8.24 (m, 4H, H-3,4), 8.06 (s, 4H, H-6), 7.81 (td, ^3J = 6 Hz, ^4J = 1 Hz, 2H, H-2), 6.05 (d, ^3J = 4 Hz, 2H, H-8), 5.76–5.69 (m, 4H, H-8,9), 5.62 (d, ^3J = 3 Hz, 1H, H-9), 5.57 (d, ^3J = 3 Hz, 1H, H-9), 2.64 (sept, ^3J = 7 Hz, 2H, H-10), 2.19 (s, 3H, H-7), 2.18 (s, 3H, H-7), 1.06–0.99 ppm (m, 12H, H-11). ^{13}C{^{1}H}DEPT-Q (100.55 MHz, acetone-d_6, *298 K*): δ 169.1 (C-5), 157.1 (C-1), 154.0 (C-4'), 153.9 (C-6'), 141.1 (C-3), 131.5 (C-4), 130.3 (C-2), 125.0 (C-6), 107.0 (C-9'), 104.9 (C-8'), 87.9–86.6 (C-8,9), 32.0 (C-10), 22.3 (C-11), 19.0 ppm (C-7). ^{31}P{^{1}H} NMR (161.85 MHz, acetone-d_6, *298 K*): δ –144.2 ppm (sept, ^3J = 703 Hz, PF_6^-). HRMS (ESI^+): *m/z* 414.0434 $[M - 2PF_6]^{2+}$ (m_{calc} = 414.0437). EA calculated for $C_{38}H_{42}Cl_2F_{12}N_4P_2Ru_2{\cdot}0.75CH_2Cl_2$: C 39.39%, H 3.71%, N 4.74%. Found: C 39.10%, H 3.93%, N 5.09%.

4.4. [N,N'-(1,4-phenylene)(bis(1-(pyridin-2-yl)(methanimine)-κ^{2}N,N') bis{chlorido(η^6-p-cymene)osmium(II)}] hexafluorophosphate *1b*

The synthesis was performed according to the general procedure using **1** (35 mg, 0.12 mmol), $[OsCl_2(cym)]_2$ (98 mg, 0.12 mmol), and NH_4PF_6 (400 mg, 2.5 mmol) to afford the product **1b** as a dark red solid (131 mg, 82%). Single crystals suitable for Xray diffraction analysis were grown by slow diffusion of toluene into a saturated solution of the complex in acetonitrile. M.p. 207–210 °C. ^{1}H NMR (399.89 MHz, acetone-d_6, *298 K*): δ 9.64 (d, ^3J = 3 Hz, 2H, H-1), 9.44 (d, ^3J = 1 Hz, 2H, H-5), 8.58–8.54 (m, 2H, H-4), 8.38 (t, ^3J = 8 Hz, 2H, H-3), 8.10 (s, 4H, H-6), 7.94–7.88 (m, 2H, H-2), 6.45 (d, ^3J = 3 Hz, 2H, H-8), 6.10 (m, 4H, H-8,9), 5.89 (d, ^3J = 3 Hz, 1H, H-9), 5.86 (d, ^3J = 3 Hz, 1H, H-9), 2.64 (sept, ^3J = 7 Hz, 2H, H-10), 2.42–2.33 (m, 6H, H-7), 1.15–1.02 ppm (m, 12H, H-11). ^{13}C{^{1}H}DEPT-Q (100.55 MHz, acetone-d_6, *298 K*): δ 170.2 (C-5), 157.0 (C-4'), 156.6 (C-1), 154.1 (C-6'), 141.1 (C-3), 131.2 (C-4), 131.0 (C-2), 125.2 (C-6), 99.5 (C-9'), 98.9 (C-8'), 79.9 (C-8), 79.2 (C-8), 77.2 (C-9), 76.8 (C-9), 32.1 (C-10), 22.5 (C-11), 18.8 ppm (C-7). ^{31}P{^{1}H} NMR (161.85 MHz, acetone-d_6, *298 K*): δ –144.2 ppm (sept, ^3J = 705 Hz, PF_6^-). HRMS (ESI^+): *m/z* 503.1021 $[M - 2PF_6]^{2+}$ (m_{calc} = 503.0980). EA calculated for $C_{38}H_{42}Cl_2F_{12}N_4P_2Os_2{\cdot}0.5NH_4PF_6$: C 33.13%, H 3.22%, N 4.58%. Found: C 33.31%, H 3.27%, N 4.73%.

4.5. [N,N'-(1,4-phenylene)(bis(1-(pyridin-2-yl)(methanimine)-κ^{2}N,N') bis{chlorido(η^5-pentamethylcyclopentadienyl)rhodium(III)}] hexafluorophosphate *1c*

The synthesis was performed according to the general procedure using **1** (98 mg, 0.34 mmol), $[RhCl_2(Cp^*)]_2$ (211 mg, 0.34 mmol), and NH_4PF_6 (1.117 g, 6.9 mmol) to afford the product **1c** as a bright yellow solid (319 mg, 82%). Single crystals suitable for X-ray diffraction analysis were grown by slow diffusion of toluene into a saturated solution of the complex in acetonitrile. M.p. 221 °C (decomp.). ^{1}H NMR (399.89 MHz, acetone-d_6, *298 K*): δ 9.23 (d, ^3J = 2 Hz, 2H, H-1), 9.13 (dd, ^3J = 4 Hz, ^4J = 1 Hz, 2H, H-5), 8.50–8.42 (m, 4H, H-3,4), 8.12–8.03 (m, 6H, H-2,6), 1.66 ppm (s, 30H, H-7). ^{13}C{^{1}H}DEPT-Q (100.55 MHz, acetone-d_6, *298 K*): δ 170.0 (C-5), 155.0 (C-4'), 154.2 (C-1), 150.5 (C-6'), 141.7 (C-3), 131.6 (C-4), 131.3 (C-2), 125.1 (C-6), 98.7 (C-7'), 9.4 ppm (C-7). ^{31}P{^{1}H} NMR (161.85 MHz, acetone-d_6, *298 K*): δ –144.3 ppm (sept, ^3J =

715 Hz, PF_6^-). HRMS (ESI^+): *m/z* 470.0887 [M – C_6H_5N – Rh(Cp*)Cl – $2PF_6$]$^+$ (mcalc = 470.0865). EA calculated for $C_{38}H_{44}Cl_2F_{12}N_4P_2Rh_2{\cdot}0.25CH_2Cl_2$: C 40.14%, H 3.92%, N 4.89%. Found: C 40.12%, H 4.24%, N 4.88%.

4.6. [N,N'-(1,4-phenylene)(bis(1-(pyridin-2-yl)(methanimine)-κ^{2}N,N') bis{chlorido(η^5-pentamethylcyclopentadienyl)iridium(III)}] hexafluorophosphate **1d**

The synthesis was performed according to the general procedure using **1** (85 mg, 0.30 mmol), $[IrCl_2(Cp^*)]_2$ (237 mg, 0.30 mmol), and NH_4PF_6 (969 mg, 5.9 mmol) to afford the product **1d** as a dark red solid (318 mg, 82%). Single crystals suitable for X-ray diffraction analysis were grown by slow diffusion of toluene into a saturated solution of the complex in acetonitrile. M.p. 242 °C (decomp.). ^{1}H NMR (399.89 MHz, acetone-*d*$_6$, *298 K*): *δ* 9.52–9.47 (m, 2H, H-5), 9.24 (d, ^3J = 3 Hz, 2H, H-1), 8.55 (d, ^3J = 5 Hz, 2H, H-3), 8.43 (td, ^3J = 7 Hz, ^4J = 1 Hz, 2H, H-4), 8.10–8.08 (m, 4H, H-6), 8.08–8.03 (m, 2H, H-2), 1.68–1.56 ppm (m, 30H, H-7). ^{13}C{^{1}H}DEPT-Q (100.55 MHz, acetone-*d*$_6$, *298 K*): *δ* 170.7 (C-5), 156.5 (C-4'), 153.3 (C-1), 151.0 (C-6'), 141.6 (C-3), 131.7 (C-2), 131.3 (C-4), 125.1 (C-6), 91.2 (C-7'), 8.6 ppm (C-7). ^{31}P{^{1}H} NMR (161.85 MHz, acetone-*d*$_6$, *298 K*): δ –144.3 ppm (sept, ^3J = 704 Hz, PF_6^-). HRMS (ESI^+): *m/z* 560.1461 [M – C_6H_5N – Ir(Cp*)Cl – $2PF_6$]$^+$ (m_{calc} = 560.1431). EA calculated for $C_{38}H_{44}Cl_2F_{12}N_4P_2Ir_2$: C 35.05%, H 3.41%, N 4.30%. Found: C 34.99%, H 3.56%, N 4.19%.

4.7. [N,N'-(methylenebis(4,1-phenylene))(bis(1-(pyridin-2-yl) (methanimine)-κ^{2}N,N')bis{chlorido(η^6-p-cymene)ruthenium(II)}] hexafluorophosphate **2a**

The synthesis was performed according to the general procedure using **2** (41 mg, 0.11 mmol), $[RuCl_2(cym)]_2$ (67 mg, 0.11 mmol), and NH_4PF_6 (352 mg, 2.2 mmol) to afford the product **2a** as a bright orange solid (100 mg, 76%). Single crystals suitable for X-ray diffraction analysis were grown by slow diffusion of toluene into a saturated solution of the complex in acetonitrile. M.p. 206–213 °C. ^{1}H NMR (399.89 MHz, acetone-*d*$_6$, *298 K*): *δ* 9.64 (d, ^3J = 3 Hz, 2H, H-1), 8.92 (d, ^3J = 3 Hz, 2H, H-5), 8.39–8.32 (m, 4H, H-3,4), 7.95–7.87 (m, 6H, H-2,6), 7.65–7.56 (m, 4H, H-7), 6.11 (d, ^3J = 3 Hz, 2H, H-12), 5.79 (d, ^3J = 3 Hz, 2H, H-11), 5.75 (d, ^3J = 3 Hz, 2H, H-12), 5.63 (d, ^3J = 3 Hz, 2H, H-11), 4.32 (s, 2H, H-8), 2.72 (sept, ^3J = 7 Hz, 2H, H-10), 2.30 (s, 6H, H-13), 1.11 ppm (d, ^3J = 4 Hz, 12H, H-9). ^{13}C{^{1}H}DEPT-Q (100.55 MHz, acetone-*d*$_6$, *298 K*): *δ* 167.7 (C-5), 156.9 (C-1), 155.9 (C-4'), 151.6 (C-6'), 144.0 (C-7'), 140.9 (C-4), 131.0 (C-7), 130.9 (C-3), 129.9 (C-2), 123.8 (C-6), 107.4 (C-11'), 104.8 (C-12'), 87.4 (C-11), 87.1 (C-12), 86.7 (C-11), 86.4 (C-12), 41.5 (C-8), 31.9 (C-10), 22.3 (C-9), 18.9 ppm (C-13). ^{31}P{^{1}H} NMR (161.85 MHz, acetone-*d*$_6$, *298 K*): δ –144.2 ppm (sept, ^3J = 705 Hz, PF_6^-). HRMS (ESI^+): *m/z* 459.0668 [M – $2PF_6$]$^{2+}$ (m_{calc} = 459.0672). EA calculated for $C_{45}H_{48}Cl_2F_{12}N_4P_2Ru_2{\cdot}1H_2O$: C 44.09%, H 4.11%, N 4.57%. Found: C 43.72%, H 4.173%, N 4.75%.

4.8. [N,N'-(methylenebis(4,1-phenylene))(bis(1-(pyridin-2-yl) (methanimine)-κ^{2}N,N')bis{chlorido(η^6-p-cymene)osmium(II)}] hexafluorophosphate **2b**

The synthesis was performed according to the general procedure using **2** (78 mg, 0.05 mmol), $[OsCl_2(cym)]_2$ (164 mg, 0.05 mmol), and NH_4PF_6 (675 mg, 0.92 mmol) to afford the product **2b** as a dark red solid (209 mg, 73%). M.p. 204–211 °C. ^{1}H NMR (399.89 MHz, acetone-*d*$_6$, *298 K*): *δ* 9.46 (d, ^3J = 3 Hz, 2H, H-1), 9.19 (d, ^3J = 3 Hz, 2H, H-5), 8.36 (d, ^3J = 3 Hz, 2H, H-4), 8.20 (td, ^3J = 6 Hz, ^4J = 1 Hz, 2H, H-3), 7.77–7.72 (m, 2H, H-2), 7.70 (dd, ^3J = 4 Hz, ^4J = 1 Hz, 4H, H-6), 7.48–7.44 (m, 4H, H-7), 6.27 (d, ^3J = 3 Hz, 2H, H-11), 5.86 (d, ^3J = 3 Hz, 2H, H-12), 5.82 (d, ^3J = 3 Hz, 2H, H-11), 5.65 (d, ^3J = 3 Hz, 2H, H-12), 4.20 (s, 2H, H-8), 2.46 (sept, ^3J = 7 Hz, 2H, H-10), 2.23 (s, 6H, H-13), 0.93 ppm (m, 12H, H-9). ^{13}C{^{1}H}DEPT-Q (100.55 MHz, acetone-*d*$_6$, *298 K*): *δ* 168.6 (C-5), 157.3 (C-4'), 156.5 (C-1), 151.6 (C-6'), 144.1 (C-7'), 141.0 (C-3), 130.9 (C-4), 130.7 (C-2), 124.2 (C-6,7), 99.0 (C-11'), 98.7 (C-12'), 79.8, (C-11) 79.2 (C-11), 77.1 (C-12), 76.9 (C-12), 41.3 (C-8), 32.1 (C-10), 22.6 (C-9), 18.8 ppm (C-13). ^{31}P{^{1}H} NMR (161.85 MHz, acetone-*d*$_6$, *298 K*): δ –144.2 ppm (sept, ^3J = 701 Hz, PF_6^-). HRMS (ESI^+): *m/z* 548.1233 [M – $2PF_6$]$^{2+}$ (m_{calc} = 548.1214). EA calculated for $C_{45}H_{48}Cl_2F_{12}N_4P_2Os_2$: C 38.99%, H 3.49%, N 4.04%. Found: C 38.86%, H 3.48%, N 4.07%.

4.9. [N,N'-(methylenebis(4,1-phenylene))(bis(1-(pyridin-2-yl) (methanimine)-κ^{2}N,N')bis{chlorido(η^5-pentamethylcyclopentadienyl) rhodium(III)}] hexafluorophosphate **2c**

The synthesis was performed according to the general procedure using **2** (110 mg, 0.07 mmol), $[RhCl_2(Cp^*)]_2$ (180 mg, 0.07 mmol), and NH_4PF_6 (954 mg, 1.5 mmol) to afford the product **2c** as a bright yellow solid (334 mg, 94%). Single crystals suitable for X-ray diffraction analysis were grown by slow diffusion of toluene into a saturated solution of the complex in acetonitrile. M.p. 198 °C (decomp.). ^{1}H NMR (399.89 MHz, acetone-*d*$_6$, *298 K*): *δ* 9.11 (d, ^3J = 3 Hz, 2H, H-1), 8.89 (s, 2H, H-5), 8.43–8.36 (m, 2H, H-3), 8.32 (d, ^3J = 5 Hz, 2H, H-4), 8.06–7.97 (m, 2H, H-2), 7.77 (d, ^3J = 5 Hz, 4H, H-6), 7.60 (d, ^3J = 4 Hz, 4H, H-7), 4.29 (s, 2H H-8), 1.55 ppm (s, 30H, H-9). ^{13}C{^{1}H}DEPT-Q (100.55 MHz, acetone-*d*$_6$, *298 K*): *δ* 168.6 (C-5), 155.7 (C-4'), 154.3 (C-1), 148.6 (C-6'), 144.6 (C-7'), 142.0 (C-3), 131.5 (C-4,7), 131.4 (C-2), 124.3 (C-6), 99.1 (C-9'), 41.9 (C-8), 9.3 ppm (C-9). ^{31}P{^{1}H} NMR (161.85 MHz, acetone-*d*$_6$, *298 K*): δ –144.3 ppm (sept, ^3J = 717 Hz, PF_6^-). HRMS (ESI^+): *m/z* 461.0757 [M – $2PF_6$]$^{2+}$ (m_{calc} = 461.0762). EA calculated for $C_{45}H_{48}Cl_2F_{12}N_4P_2Rh_2{\cdot}0.5CH_2Cl_2$: C 43.51%, H 4.09%, N 4.46%. Found: C 43.42%, H 4.05%, N 4.49%.

4.10. [N,N'-(methylenebis(4,1-phenylene))(bis(1-(pyridin-2-yl) (methanimine)-κ^{2}N,N')bis{chlorido(η^5-pentamethylcyclopentadienyl) iridium(III)}] hexafluorophosphate **2d**

The synthesis was performed according to the general procedure using **2** (66 mg, 0.06 mmol), $[IrCl_2(Cp^*)]_2$ (139 mg, 0.06 mmol), and NH_4PF_6 (567 mg, 1.2 mmol) to afford the product **2d** as a red solid (210 mg, 87%). M.p. 222–232 °C. ^{1}H NMR (399.89 MHz, acetone-*d*$_6$, *298 K*): *δ* 9.34 (s, 2H, H-5), 9.18 (d, ^3J = 3 Hz, 2H, H-1), 8.50 (d, ^3J = 5 Hz, 2H, H-4), 8.38 (td, ^3J = 8 Hz, ^4J = 1 Hz, 2H, H-3), 8.03–7.99 (m, 2H, H-2), 7.79–7.75 (m, 4H, H-6), 7.60 (dd, ^3J = 4 Hz, ^4J = 1 Hz, 4H, H-7), 4.30 (s, 2H, H-8), 1.55 ppm (s, 30H, H-9). ^{13}C{^{1}H}DEPT-Q (100.55 MHz, acetone-*d*$_6$, *298 K*): *δ* 169.0 (C-5), 156.9 (C-4'), 153.3 (C-1), 148.6 (C-6'), 144.1 (C-7'), 141.5 (C-3), 131.4 (C-2), 130.9 (C-4,7), 123.9 (C-6), 91.3 (C-9'), 41.4 (C-8), 8.6 ppm (C-9). ^{31}P{^{1}H} NMR (161.85 MHz, acetone-*d*$_6$, *298 K*): δ –144.4 ppm (sept, ^3J = 715 Hz, PF_6^-). HRMS (ESI^+): *m/z* 551.1333 [M – $2PF_6$]$^{2+}$ (m_{calc} = 551.1319). EA calculated for $C_{45}H_{48}Cl_2F_{12}N_4P_2Ir_2{\cdot}0.5CH_2Cl_2$: C 38.09%, H 3.58%, N 3.91%. Found: C 37.89%, H 3.48%, N 3.96%.

4.11. DMSO and aqueous stability studies

DMSO Stability studies were conducted by dissolving *ca.* 1 mg of the complex in DMSO-*d*$_6$ (0.5 mL). ^{1}H NMR spectra were recorded at *t* = 0, 2, 6, 24, 48, and 72 h to determine compound stability in 100% DMSO.

Hydrolysis stability studies were conducted similarly by dissolving *ca.* 1 mg of the complex in DMSO-*d*$_6$ (0.05 mL) and diluting it with D_2O (0.45 mL) to form a 10% DMSO-*d*$_6$/D_2O solution. ^{1}H NMR spectra were recorded at *t* = 0, 2, 6, 24, 48, and 72 h to determine the stability of the complex in aqueous solutions, as modelled by D_2O. After 72 h, $AgNO_3$ (2 equiv.) was added to force hydrolysis. After vigorous shaking, the yellow suspension was filtered and a ^{1}H NMR spectrum of the filtrate was recorded for the hydrolyzed complex as a comparison to the previous samples. In addition, compounds that demonstrated reasonable levels of hydrolysis over the first 6 h were tested by the addition of 100

mM NaCl in D_2O (0.45 mL) to a solution of *ca.* 1 mg of the complex in DMSO-d_6 (0.05 mL) to approximate the standard [Cl^-] in blood.

4.12. Reactivity studies with biomolecules

The biomolecule interactions of complexes with 9-ethylguanine (EtG, AK Scientific, 98%), L-methionine (Met), L-histidine (His) and L-cysteine (Cys) were studied by ^{1}H NMR spectroscopy. Stock solutions of EtG, His, Cys, or Met (2 equiv.) in D_2O (0.25 mL) were added to a solution of *ca.* 1 mg of **1a** in DMSO-d_6 (0.05 mL) and D_2O (0.2 mL) to form a 10% DMSO-d_6/D_2O solution. ^{1}H NMR spectra were recorded over a time period of 72 h.

4.13. Cell cytotoxicity studies

HCT116, SW480 and NCI-H460 cells were supplied by ATCC, while SiHa cells were supplied by Dr. David Cowan, Ontario Cancer Institute, Canada. The cells were grown in α-MEM supplemented with 5% FCS at 37 °C in a humidified incubator with 5% CO_2. Cells were seeded at 750 (HCT116, NCI-H460), 4000 (SiHa) and 5000 (SW480) cells per well in 96-well plates and left to settle for 24 h. Compounds were added to the plates in a series of 3-fold dilutions in 0.5% DMSO at the highest concentration for 72 h before the assay was terminated by addition of 10% trichloroacetic acid (Merck Millipore) at 4 °C for 1 h. Cells were stained with 0.4% sulforhodamine B (Sigma-Aldrich) in 1% acetic acid for 30 min in the dark at room temperature and then washed with 1% acetic acid to remove any unbound dye. The stain was dissolved in unbuffered Tris base (10 mM; Serva) for 30 min on a plate shaker in the dark and quantitated on a BioTek EL808 microplate reader at an absorbance of 490 nm, with a reference wavelength of 450 nm, to determine the percentage of cell-growth inhibition by determining the absorbance of each sample relative to a negative (no inhibitor) and a no-growth control (day 0). IC_{50} values were calculated with SigmaPlot 12.5 (Systat Software Inc.) using a three-parameter logistic sigmoidal dose–response curve between the calculated growth inhibition and the compound concentration. The presented IC_{50} values are the mean of at least 3 independent experiments, where 10 concentrations were tested in duplicate for each compound.

CRediT authorship contribution statement

Tasha R. Steel: Synthesis and characterization, In vitro cytotoxicity, Writing - original draft preparation. **Kelvin K.H. Tong:** In vitro cytotoxicity. **Tilo Söhnel:** Crystallography. **Stephen M.F. Jamieson:** In vitro cytotoxicity. **L. James Wright:** Conceptualization, Supervision. **James D. Crowley:** Conceptualization. **Muhammad Hanif:** Supervision, Synthesis. **Christian G. Hartinger:** Supervision, Conceptualization, Writing - review & editing. All the authors contributed to the drafting of the manuscript and have agreed to the submission.

Declaration of Competing Interest

The authors declare that they have no known competing financial interests or personal relationships that could have appeared to influence the work reported in this paper.

Acknowledgements

We would like to thank the University of Auckland and the Marsden Fund Council, managed by the Royal Society Te Apārangi. T.R.S. & K.K. H.T. thank the University of Auckland for University of Auckland Doctoral Scholarships. We are grateful to Tanya Groutso for collecting the X-ray diffraction, and to Tony Chen and Mansa Nair for collecting the MS data.

Appendix A. Supplementary data

Supplementary data to this article can be found online at https://doi.org/10.1016/j.ica.2020.120220.

References

[1] B. Rosenberg, Cisplatin: its history and possible mechanisms of action, in: A. W. Prestayko, S.T. Crooke, S.K. Carter (Eds.), Cisplatin: Current Status and New Developments, Academic Press Inc, New York, 1980, pp. 9–20.
[2] L. Kelland, Nat. Rev. Cancer 7 (2007) 573.
[3] M. Hanif, C.G. Hartinger, Future Med. Chem. 10 (2018) 615–617.
[4] M.A. Jakupec, M. Galanski, V.B. Arion, C.G. Hartinger, B.K. Keppler, Dalton Trans. (2008) 183–194.
[5] A. Bhargava, U.N. Vaishampayan, Expert Opin. Invest. Drugs 18 (2009) 1787–1797.
[6] N. Shah, D.S. Dizon, (2009).
[7] R.R. Crichton, Biological Inorganic Chemistry: A New Introduction to Molecular Structure and Function, Elsevier, 2012.
[8] G.Y. Ho, N. Woodward, J.I. Coward, Crit. Rev. Oncol. Hematol. 102 (2016) 37–46.
[9] D.M. Cheff, M.D. Hall, J. Med. Chem. 60 (2017) 4517–4532.
[10] M. Hanif, M.V. Babak, C.G. Hartinger, Drug Discov. Today 19 (2014) 1640–1648.
[11] M.G. Mendoza-Ferri, C.G. Hartinger, A.A. Nazarov, R.E. Eichinger, M.A. Jakupec, K. Severin, B.K. Keppler, Organometallics 28 (2009) 6260–6265.
[12] C.G. Hartinger, A.D. Phillips, A.A. Nazarov, Curr. Top. Med. Chem. 11 (2011) 2688–2702.
[13] É.A. Enyedy, O. Dömötör, C.M. Hackl, A. Roller, M.S. Novak, M.A. Jakupec, B. K. Keppler, W. Kandioller, J. Coord. Chem. 68 (2015) 1583–1601.
[14] B.T. Elie, J. Fernández-Gallardo, N. Curado, M.A. Cornejo, J.W. Ramos, M. Contel, Eur. J. Med. Chem. 161 (2019) 310–322.
[15] S. Komeda, T. Moulaei, K.K. Woods, M. Chikuma, N.P. Farrell, L.D. Williams, J. Am. Chem. Soc. 128 (2006) 16092–16103.
[16] D. Jodrell, T. Evans, W. Steward, D. Cameron, J. Prendiville, C. Aschele, C. Noberasco, M. Lind, J. Carmichael, N. Dobbs, Eur. J. Cancer 40 (2004) 1872–1877.
[17] M.-G. Mendoza-Ferri, C.G. Hartinger, R.E. Eichinger, N. Stolyarova, K. Severin, M. A. Jakupec, A.A. Nazarov, B.K. Keppler, Organometallics 27 (2008) 2405–2407.
[18] M.G. Mendoza-Ferri, C.G. Hartinger, M.A. Mendoza, M. Groessl, A.E. Egger, R. E. Eichinger, J.B. Mangrum, N.P. Farrell, M. Maruszak, P.J. Bednarski, J. Med. Chem. 52 (2009) 916–925.
[19] L.K. Batchelor, E. Păunescu, M.N. Soudani, R. Scopelliti, P.J. Dyson, Inorg. Chem. 56 (2017) 9617–9633.
[20] G.E. Davey, Z. Adhireksan, Z. Ma, T. Riedel, D. Sharma, S. Padavattan, D. Rhodes, A. Ludwig, S. Sandin, B.S. Murray, Nat. Commun. 8 (2017) 1575.
[21] A.A. Nazarov, M.-G. Mendoza-Ferri, M. Hanif, B.K. Keppler, P.J. Dyson, C. G. Hartinger, J. Biol. Inorg. Chem. 23 (2018) 1159–1164.
[22] S.D. Fairbanks, C.C. Robertson, F.R. Keene, J.A. Thomas, M.P. Williamson, J. Am. Chem. Soc. 141 (2019) 4644–4652.
[23] L. Boselli, M.L. Carraz, S. Mazères, L. Paloque, G.N. González, F.O. Benoit-Vical, A. Valentin, C. Hemmert, H. Gornitzka, Organometallics 34 (2015) 1046–1055.
[24] B.T. Elie, Y. Pechenyy, F. Uddin, M. Contel, J. Biol. Inorg. Chem. 23 (2018) 399–411.
[25] M. Auzias, J. Gueniat, B. Therrien, G. Süss-Fink, A.K. Renfrew, P.J. Dyson, J. Organomet. Chem. 694 (2009) 855–861.
[26] F. Pelletier, V. Comte, A. Massard, M. Wenzel, S. Toulot, P. Richard, M. Picquet, P. Le Gendre, O. Zava, F. Edafe, J. Med. Chem. 53 (2010) 6923–6933.
[27] O. Nováková, A.A. Nazarov, C.G. Hartinger, B.K. Keppler, V. Brabec, Biochem. Pharmacol. 77 (2009) 364–374.
[28] S. Movassaghi, E. Leung, M. Hanif, B.Y.T. Lee, H.U. Holtkamp, J.K.Y. Tu, T. Söhnel, S.M.F. Jamieson, C.G. Hartinger, Inorg. Chem. 57 (2018) 8521–8529.
[29] S. Parveen, M. Hanif, E. Leung, K.K. Tong, A. Yang, J. Astin, G.H. De Zoysa, T. R. Steel, D. Goodman, S. Movassaghi, Chem. Commun. 55 (2019) (2019) 12016–12019.
[30] H. Chen, J.A. Parkinson, O. Nováková, J. Bella, F. Wang, A. Dawson, R. Gould, S. Parsons, V. Brabec, P.J. Sadler, Proc. Natl. Acad. Sci. 100 (2003) 14623–14628.
[31] R. Hernandez-Molina, A. Mederos, Science (2003) 411–446.
[32] W. Zishen, G. Ziqi, Y. Zhenhuan, Synth. React. Inorg. Met.-Org. Chem. 20 (1990) 335–344.
[33] Z.-Y. Yang, R.-D. Yang, F.-S. Li, K.-B. Yu, Polyhedron 19 (2000) 2599–2604.
[34] M.A. Ali, A.H. Mirza, R.J. Butcher, M. Tarafder, T.B. Keat, A.M. Ali, J. Inorg. Biochem. 92 (2002) 141–148.
[35] P. Wu, D.L. Ma, C.H. Leung, S.C. Yan, N. Zhu, R. Abagyan, C.M. Che, Chem. Eur. J. 15 (2009) 13008–13021.
[36] X. Qiao, Z.-Y. Ma, C.-Z. Xie, F. Xue, Y.-W. Zhang, J.-Y. Xu, Z.-Y. Qiang, J.-S. Lou, G.-J. Chen, S.-P. Yan, J. Inorg. Biochem. 105 (2011) 728–737.
[37] J. Zhao, S. Li, X. Wang, G. Xu, S. Gou, Inorg. Chem. 58 (2019) 2208–2217.
[38] N.M. Shavaleev, Z.R. Bell, G. Accorsi, M.D. Ward, Inorg. Chim. Acta 351 (2003) 159–166.
[39] M.C. Young, A.M. Johnson, A.S. Gamboa, R.J. Hooley, Chem. Commun. 49 (2013) 1627–1629.
[40] A. Singh, M. Chandra, A.N. Sahay, D.S. Pandey, K.K. Pandey, S.M. Mobin, M. C. Puerta, P. Valerga, J. Organomet. Chem. 689 (2004) 1821–1834.
[41] R. Lang, K. Polborn, T. Severin, K. Severin, Inorg. Chim. Acta 294 (1999) 62–67.

[42] C.R. Groom, I.J. Bruno, M.P. Lightfoot, S.C. Ward, Acta Crystallogr Sect. B: Struct. Sci. 72 (2016) 171–179.
[43] A.F. Peacock, M. Melchart, R.J. Deeth, A. Habtemariam, S. Parsons, P.J. Sadler, Chem. Eur. J. 13 (2007) 2601–2613.
[44] M. Patra, T. Joshi, V. Pierroz, K. Ingram, M. Kaiser, S. Ferrari, B. Spingler, J. Keiser, G. Gasser, Chem. Eur. J. 19 (2013) 14768–14772.
[45] M.D. Hall, K.A. Telma, K.-E. Chang, T.D. Lee, J.P. Madigan, J.R. Lloyd, I. S. Goldlust, J.D. Hoeschele, M.M. Gottesman, Cancer Res. 74 (2014) 3913–3922.
[46] F. Wang, H. Chen, S. Parsons, I.D. Oswald, J.E. Davidson, P.J. Sadler, Chem. Eur. J. 9 (2003) 5810–5820.
[47] B. Rosenberg, L. Van Camp, T. Krigas, Nature 205 (1965) 698–699.
[48] H. Sigel, Chem. Soc. Rev. 22 (1993) 255–267.
[49] M.-H. Baik, R.A. Friesner, S.J. Lippard, J. Am. Chem. Soc. 125 (2003) 14082–14092.
[50] A. Robertazzi, J.A. Platts, J. Biol. Inorg. Chem. 10 (2005) 854–866.
[51] M. Kubanik, H. Holtkamp, T. Söhnel, S.M. Jamieson, C.G. Hartinger, Organometallics 34 (2015) 5658–5668.
[52] W. Kandioller, C.G. Hartinger, A.A. Nazarov, C. Bartel, M. Skocic, M.A. Jakupec, V. B. Arion, B.K. Keppler, Chem. Eur. J. 15 (2009) 12283–12291.
[53] M. Hanif, H. Henke, S.M. Meier, S. Martic, M. Labib, W. Kandioller, M.A. Jakupec, V.B. Arion, H.-B. Kraatz, B.K. Keppler, C.G. Hartinger, Inorg. Chem. 49 (2010) 7953–7963.
[54] W.D. Tremlett, K.K. Tong, T.R. Steel, S. Movassaghi, M. Hanif, S.M. Jamieson, T. Söhnel, C.G. Hartinger, J. Inorg. Biochem. 199 (2019), 110768.
[55] M.A. Bennett, A.K. Smith, J. Chem. Soc., Dalton Trans. (1974) 233–241.
[56] A.F. Peacock, A. Habtemariam, S.A. Moggach, A. Prescimone, S. Parsons, P. J. Sadler, Inorg. Chem. 46 (2007) 4049–4059.
[57] C. White, A. Yates, P. Maitlis, D. Heinekey, Inorg. Synth. (1992) 228–234.
[58] P.S. Nejman, B. Morton-Fernandez, D.J. Moulding, K.S.A. Arachchige, D.B. Cordes, A.M. Slawin, P. Kilian, J.D. Woollins, Dalton Trans. 44 (2015) 16758–16766.
[59] M. Jakoobi, N. Halcovitch, G.F. Whitehead, A.G. Sergeev, Angew. Chem., Int. Ed. Engl. 129 (2017) 3314–3317.
[60] G.M. Sheldrick, Acta Crystallogr. Sect. A: Found. Crystallogr. 64 (2008) 112–122.
[61] O.V. Dolomanov, L.J. Bourhis, R.J. Gildea, J.A. Howard, H. Puschmann, J. Appl. Crystallogr. 42 (2009) 339–341.
[62] L.J. Bourhis, O.V. Dolomanov, R.J. Gildea, J.A. Howard, H. Puschmann, Acta Crystallogr. Sect. A: Found. Adv. 71 (2015) 59–75.